ELSEVIER

A new multiprobe method of roundness measurements

Wei Gao, Satoshi Kiyono, and Tadatoshi Nomura
Department of Mechatronics, Faculty of Engineering, Tohoku University, Aoba-ku, Sendai, Japan

This paper presents a new multiprobe method for roundness measurements called the mixed method. In this method, displacements at two points on a cylindrical workpiece and an angle at one of the two points are simultaneously monitored by two probes. The differential output of the probes cancels the effect of the spindle error, and deconvolving the differential data yields the correct roundness error. The mixed method is compared to the traditional 3-point method with respect to the transfer function and resolution. Unlike the 3-point method, the mixed method can completely separate the roundness error and the spindle error, and can measure high-frequency components regardless of the probe distance. Resolution can also be improved throughout the entire frequency domain by increasing angular separation of the probes. An optical sensor specifically suited to the mixed method is designed and used to make roundness measurements. A fiber coupler and single-mode fibers are used in the sensor to divide a light beam from a laser diode into two beams, resulting in a compact sensor with good thermal drift characteristics. The displacement meter of the sensor is based on the imaging system principle and has a resolution of 0.1 μm. The angle meter is based on the principle of autocollimation and has a resolution of 0.5 in. A measurement system is constructed to realize measurements of roundness by using the optical sensor. Experimental results confirming the effectiveness of the mixed method for roundness measurements are also presented in this paper.

Keywords: *metrology; on-machine measurement; roundness; spindle error; multiprobe method; mixed method; 3-point method; resolution; optical sensor*

Introduction

To measure roundness errors of cylindrical workpieces and spindle errors of machine tools in on-machine conditions, it is important to separate the roundness error and spindle error from each other. Basically, there are two kinds of error separation methods.[1] One is known as the multiorientation method,[2–4] and the other is the multiprobe method.[5–14] Multiorientation methods including the step method[2] and the reversal method[3,4] can separate the spindle error and the roundness error effectively, if the spindle error has good repeatability. Compared with multiorientation methods, multiprobe methods are more suitable for on-machine measurements, because the repeatability of the spindle error is not necessary. In multiprobe methods, the 3-point method[7–12] is the most widely used one. The 3-point method uses three displacement probes to detect roundness error and two-dimensional (2-D) spindle error components simultaneously. The effect of the spindle error is cancelled in the differential output of the probes, and a deconvolving operation on the differential data yields the correct roundness error. However, some high-frequency components cannot be measured accurately with this method. It should be pointed out that this problem exists in other multiprobe methods.

To overcome this drawback of the 3-point method when used for roundness measurements,

Address reprint requests to Wei Gao, Kiyono Labroatory, Department of Metatronics, Tokohu University, Aramaki A2A A0BA, Aoba-Ku, Sendai 980, Japan.

Precision Engineering 19:37–45, 1996

655 Avenue of the Americas, New York, NY 10010

0141-6359/96/$15.00
PII S0141-6359(96)00006-2

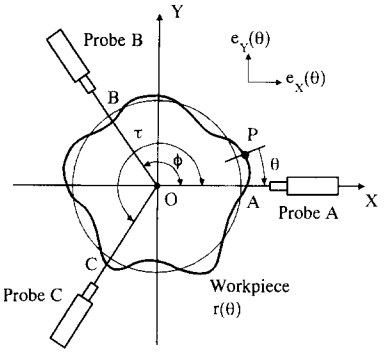

Figure 1 Principle of the 3-point method

we investigated the possibility of applying the mixed method[15] that was developed for measurements of straightness. This method uses two displacement probes and one angle probe to separate the roundness error from the spindle error completely and to capture high-frequency components.

In this paper, characteristics of this new multiprobe method for roundness measurements are investigated and compared with the 3-point method. An experimental optical sensor was fabricated for use in the mixed method. A measurement system with the optical sensor was also constructed, and roundness errors of cylindrical mirrors were measured. The effectiveness of the mixed method for roundness measurements is confirmed by the experimental results.

The 3-point method and the mixed method

Measurement principle

Figure 1 gives the principle of the 3-point method schematically. Three probes, which are fixed around a cylindrical workpiece, scan it while it is rotating. Assume that point O is the intersection of the three probes and is near the rotational center of the workpiece. The fixed coordinate axes *X–Y* are also shown in the same figure. Let *P* be a representative point of the workpiece and the roundness error be described by the function $r(\theta)$, where θ is the angle between point *P* and the *Y*-axis. Let ϕ and τ be the angles between probes.

If the displacement outputs of the probes are

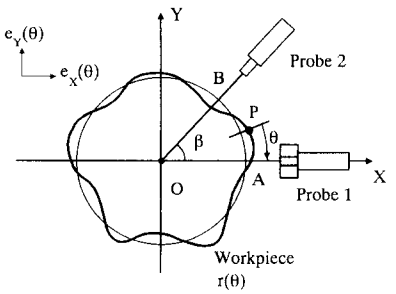

Figure 2 Principle of the mixed method

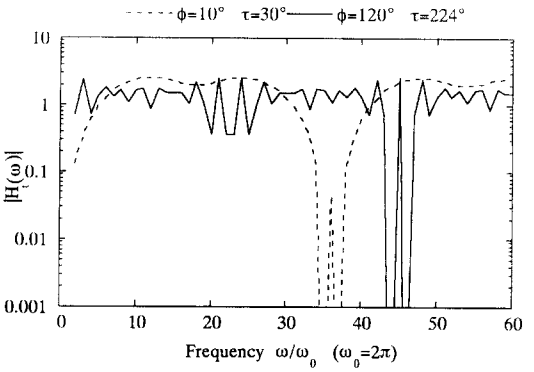

Figure 3 Transfer function of the 3-point method

denoted by $m_A(\theta)$,$m_B(\theta)$, and $m_c(\theta)$, respectively, the outputs can be expressed as:

$$m_A(\theta) = r(\theta) + e_X(\theta) \quad (1)$$

$$m_c(\theta) = r(\theta - \phi) + e_Y(\theta) \cdot \sin\phi + e_X(\theta) \cdot \cos\phi \quad (2)$$

$$m_c(\theta) = r(\theta - \tau) + e_Y(\theta) \cdot \sin\tau + e_X(\theta) \cdot \cos\tau \quad (3)$$

where $e_X(\theta)$ and $e_Y(\theta)$ are the *X*-directional component and *Y*-directional component of the spindle error, respectively. R_r is the radius of the workpiece.

The differential output $m_t(\theta)$ of the 3-point method can be denoted as

$$m_t(\theta) = m_A(\theta) + a \cdot m_B(\theta) + b \cdot m_C(\theta) = r(\theta) + a \cdot r(\theta - \phi) + b \cdot r(\theta - \tau) \quad (4)$$

where

$$a = \sin\tau/\sin(\tau - \phi) \quad (5)$$

$$b = \sin\phi/\sin(\tau - \phi) \quad (6)$$

Consequently, the spindle error is cancelled.

The principle of the mixed method is shown in *Figure 2*. Two probes are used in this method. Let the displacement output and the angle output of probe 1 be $m_1(\theta)$ and $\mu_1(\theta)$, and the displacement output of probe 2 be $m_2(\theta)$, then

$$m_1(\theta) = r(\theta) + e_X(\theta) \quad (7)$$

$$\mu_1(\theta) = (dr(\theta)/d\theta)R_r + e_Y(\theta)/R_r \quad (8)$$

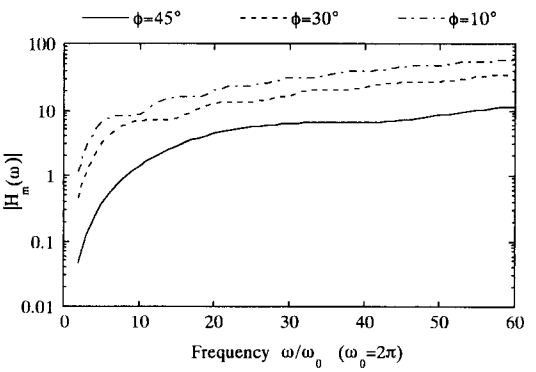

Figure 4 Transfer function of the mixed method

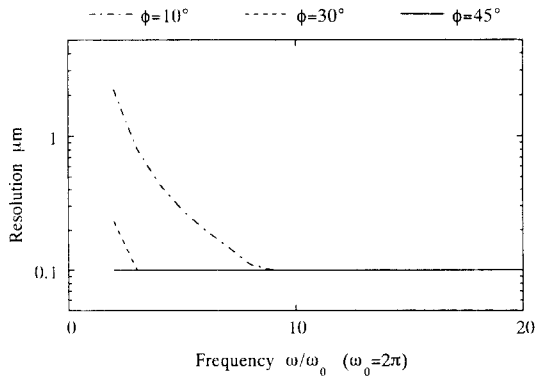

Figure 5 Resolution of the mixed method

$$m_2(\theta) = r(\theta - \beta) + e_Y(\theta) \cdot \sin\beta + e_X(\theta) \cdot \cos\beta \quad (9)$$

where β is the angle between the probes.

There are three unknown variables in the output data of the probes shown in Equations (7–9). They are $r(\theta)$, $e_X(\theta)$, and $e_Y(\theta)$. The roundness error $r(\theta)$ can be separated from $e_X(\theta)$ and $e_Y(\theta)$ by using the three output data of the probes. The differential output $m_m(\theta)$ of the mixed method, in which the spindle error is cancelled, can be given by

$$\begin{aligned} m_m(\theta) &= m_1(\theta) - m_2(\theta)/\cos\beta - R_r \cdot \tan\beta \cdot \mu_1(\theta) \\ &= r(\theta) - r(\theta - \beta)/\cos\beta - \tan\beta \cdot (dr(\theta)/d\theta) \end{aligned} \quad (10)$$

Transfer function

Let us consider Equation (4) as a system. In this system, $r(\theta)$ is treated as the input and $m_t(\theta)$ as the output. According to the theory of digital filters,[16,17] the relation between the input $r(\theta)$ and the output $m_t(\theta)$ can be defined by the following transfer function of the 3-point method:

$$\begin{aligned} H_t(\omega) &= M_t(\omega)/R(\omega) \\ &= 1 + a \cdot e^{-j\omega\phi} + b \cdot e^{-j\omega\tau} \end{aligned} \quad (11)$$

where ω is the spatial frequency, and $M_t(\omega)$ and $R(\omega)$ are the fast Fourier transforms (FFT) of $m_t(\theta)$ and $r(\theta)$, respectively. $R(\omega)$ can be obtained from $M_t(\omega)$ and $H(\omega)$, and $r(\theta)$ can be evaluated by IFFT of $R(\omega)$.

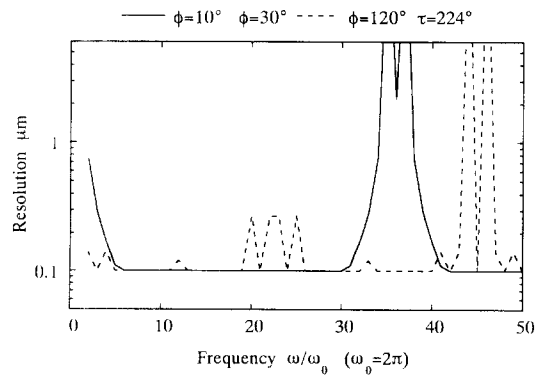

Figure 6 Resolution of the 3-point method

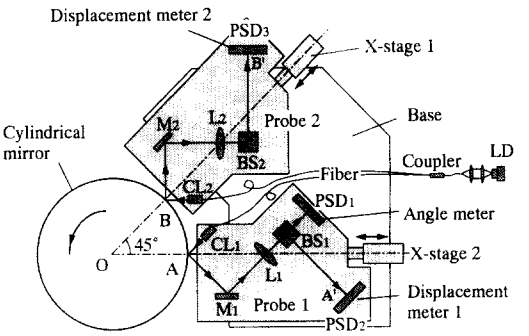

Figure 7 Optical sensor for the mixed method

The transfer function of the mixed method can be expressed as follows:

$$\begin{aligned} H_m(\omega) &= M_m(\omega)/R(\omega) \\ &= 1 - e^{-j\omega\beta}/\cos\beta - j\omega\tan\beta \end{aligned} \quad (12)$$

where $M_m(\omega)$ and $R(\omega)$ are the Fourier transforms of $m_m(\theta)$ and $r(\theta)$, respectively.

Taking the angles between probes as parameters, transfer functions $H_t(\omega)$ and $H_m(\omega)$ are shown in *Figures 3* and *4*, respectively. In the 3-point method, the amplitude at some frequencies in the transfer function approaches zero. This prevents the 3-point method from measuring the corresponding frequency components correctly. Such zero points are not found in the transfer function of the mixed method. This means that the mixed method is superior when high-frequency components of the roundness error and the spindle error are important, as for example, on-machine measurements.

Resolution

The resolution of the 3-point method and the mixed method can be evaluated by calculating the resolution of each spatial frequency component in the measured roundness error.

Figure 5 shows the resolution of the mixed method, where the resolution of the displacement

Table 1 Specifics of devices in *Figure 7*

M_1, M_2	Flat mirror, size: 10 mm × 10 mm
BS_1, BS_2	Beam splitter, size: 10 mm × 10 mm × 10 mm
L_1, L_2	Cylindrical lens, Diameter 10 mm, focal distance 30 mm
PSD_1, PSD_2, PSD_3	Position-sensing detector (Hamamatsu Hotonics S3979), sensitive area 3 mm × 1 mm (one dimension), resolution: 0.1 μm

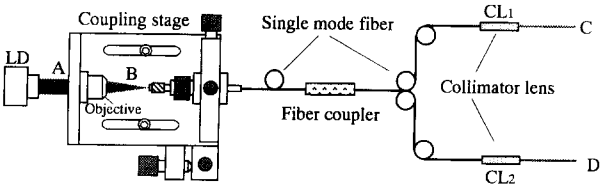

Figure 8 Optical fiber system for power transmission

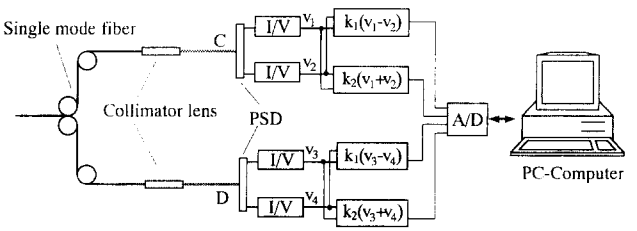

Figure 9 Experimental setup for investigating the stability of the fiber output

meter and angle meter are taken to be 0.1 μm and 0.5 in., respectively. The angles between probes are taken as parameters. It can be seen from *Figure 5* that the resolution of the mixed method is almost the same as that of the displacement meter. In the low-frequency range, resolution improves as β increases. The resolution throughout the entire frequency range approaches that of the displacement meter when $\beta \geqslant 45°$.

The resolution of the 3-point method is shown in *Figure 6*. There are some low-resolution components in the 3-point method attributable to the zero points in the transfer function. In addition, the resolution of the mixed method when $\beta = 30°$ is much higher than that of the 3-point method when $(\phi,\tau) = (10°, 30°)$, which requires nearly the same angular distance for the spatial arrangement of the probes.

Optical sensor

Structure of the optical sensor

Figure 7 shows the optical sensor developed for roundness measurements with the mixed method. *Table 1* shows the specifics of the devices in *Figure 7*. To improve the resolution of the mixed method, the angular distance between the probes is set to 45°. The probes are mounted on individual stages so that their positions relative to the cylindrical mirror can be adjusted.

In the multiprobe methods using optical probes, matching of the characteristics of the power sources of the probes is vitally important. For this purpose, an optical fiber system with a fiber coupler and single mode fibers is used to splitting the light from one source into two beams that are used as the power sources of the probes.

The collimated beams from the fiber system are projected onto points *A* and *B* on the measured surface. The reflected beams from points *A* and *B* are reflected again by the flat mirrors M_1 and M_2, and then accepted by the angle meter and the displacement meters. The angle meter utilizes the principle of autocollimation. It consists of lens L_1 and position-sensing detector PSD_1 placed at the focal position of L_1. The displacement meters use image formation systems in which points *A'* and *B'* on PSD_2 and PSD_3 are the image points of points *A* and *B*. The displacement meter 1 and the angle meter use the same lens L_1 for compactness of the structure. Probe resolution and measurement

Table 2 Specifics of devices in *Figure 8*

LD (laser diode)	Sharp LT022MD, output power 5 mW (maximum), wavelength 780 nm
Coupling stage	Newport MF915, objective: diameter 7 mm, Focal distance 25.5 mm
Fiber coupler and single-mode fiber, CL_1, CL_2 (Collimator lens)	Acrotec 780-H-50/ 50-R-NC, NA of the fiber: 0.1 NSG OPAL-M-W1825-125-085, diameter 1.8 mm, focal distance: 1.85 mm

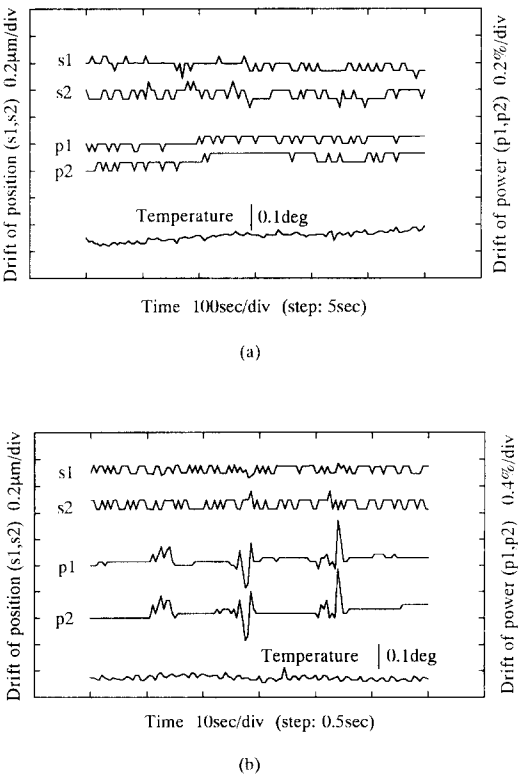

Figure 10 Stability of the fiber output

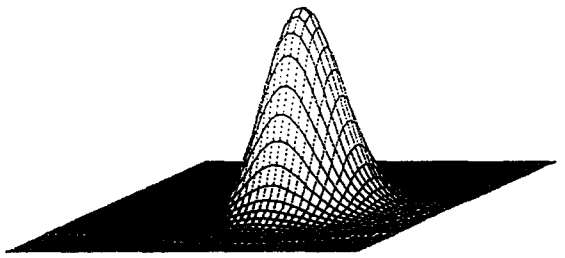

(a) 3-D expression

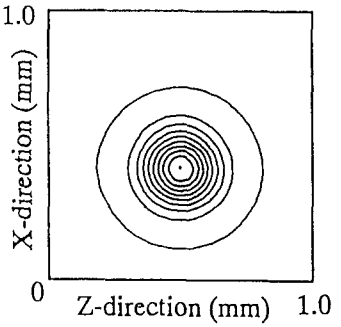

(b) Contour expression

Figure 11 Intensity distribution of the fiber output

range are determined by the performance of the PSD, the focal length of the lens, and the relative position of the lens and PSD. In these experiments, the focal length of the objective is 30 mm, and the magnification of the displacement meter is 1. Given that the resolution of the PSD is 0.1 μm, the resolution of the probes is determined to be 0.07 μm and 0.34 in.

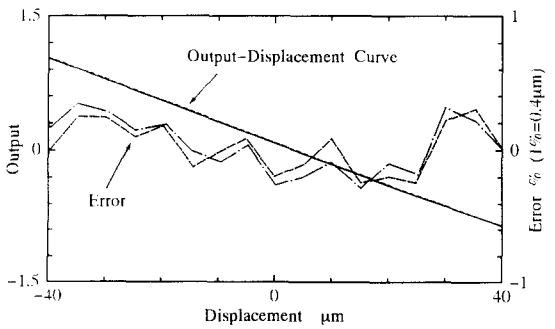

Figure 12 Calibrated results of the displacement meter

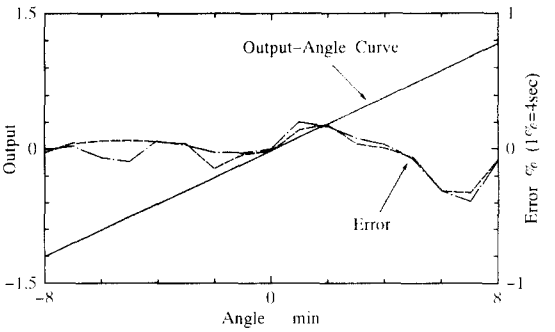

Figure 13 Calibrated results of the angle meter

Optical fiber system for power transmission

Figure 8 shows the optical fiber system. *Table 2* shows the specifics of devices in *Figure 8*. The stability of the fiber output is investigated by the experimental setup shown in *Figure 9*. According to the charaacteristics of the PSD, *s1* and *s2* expressed in Equations (13,14) show the stability of the positions of the sports at points *C* and *D* in *Figure 8* and *p*1 and *p*2 expressed in Equations (15,16) show the stability of the intensity level. To ensure the performance of the sensor, *s*1 and *s*2 must be stable. It should be pointed out that basically, the stability of the intensity level does not affect the performance of the sensor.

$$s1 = k_1(v_1 - v_2)I/k_2(v_1 + v_2) \quad (13)$$

$$s2 = k_1(v_3 - v_4)I/k_2(v_3 + v_4) \quad (14)$$

$$p1 = k_2(v_1 + v_2) \quad (15)$$

$$p2 = k_2(v_3 + v_4) \quad (16)$$

Figure 10 shows the measured results. It can be found from *Figure 10a* that the stability of the positions of the spots is better than 0.1 μm, which is within the limitation estimated from the signal to noise ratio of the experimental system. It can also be seen that the stability of the intensity is better than 0.1%. Figure 10b shows the measurement result when the fiber is shaken repeatedly. It can be seen that *s1, s2,* remains stable while *p1, p2* varies with the shaking.

Figure 11 shows the measured intensity distribution of the output beam, where (a) is the three-dimensional (3-D) expression, and (b) is the contour expression. The intensity of the output beam

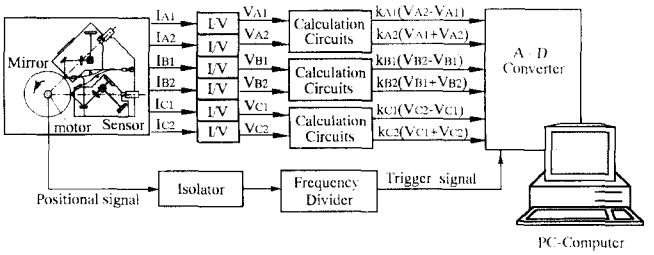

Figure 14 Measurement system

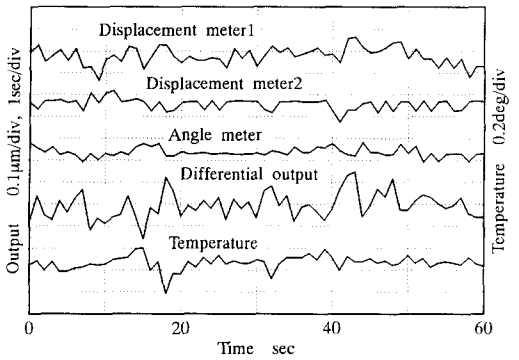

Figure 15 Thermal drift of the sensor in short term

seems to have a Gaussian distribution, which is the typical distribution of laser beams.

These results confirmed that the optical fiber system for power transmission has good performance when used as the power source for the new optical sensor.

Basic performance of the optical sensor

A capacitance type displacement sensor (Microsense) was used to calibrate the newly developed displacement meters in a range of ±40 μm. *Figure 12* shows calibration result obtained in two separate measurements. The fitting error to linear approximation is about 0.2 μm.

A photoelectric autocollimator with a resolution of 0.1 in. was used to calibrate the angle meter in a calibration range of ±8 ft. *Figure 13* shows the calibration results. The fitting error to linear approximation is about 3 in. Estimating from the signal-to-noise ratio, the resolution of the displacement meters is about 0.1 μm, and that of the angle meter is about 0.5 in.

Measurement system

Figure 14 shows the system for roundness measurements. The sensor is fixed, and the cylindrical mirror is driven by a servomotor with an optical encoder. The profile of the mirror can be sampled by the probes with an equal sampling interval

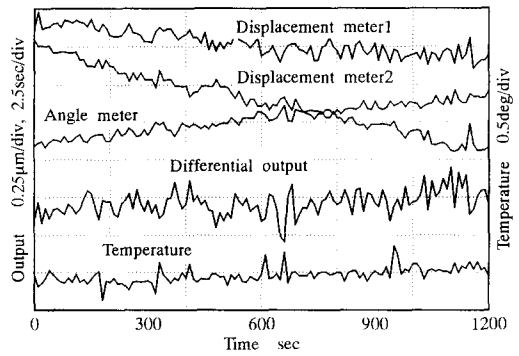

Figure 16 Thermal drift of the sensor in long term

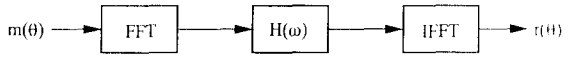

Figure 17 Procedure of data processing in the mixed method

given by the encoder when the mirror is rotating. A ball bearing is used in the spindle.

There are two displacement meters and one angle meter in the sensor, and two current output signals from the PSD of each probe. The output signals are changed to voltage output signals by *I–V* converter circuits. Then the two voltage output signals of each PSDs are calculated to determine the position of the optical spot on the PSD by a calculation circuit. The output signals of the calculation circuits are taken into a personal computer via a 12-bit A/D converter. The output signals are sampled simultaneously so that the errors attributable to the sampling time delay can be avoided.

The positional signal of the optical encoder of the servomotor is sent to the A/D converter as a trigger signal. An isolating circuit is used to isolate the noise in the positional signal from the A/D converter, because the noise in the positional signal is too large. In addition, a frequency divider circuit is used to change the decimal output of the optical encoder to a binary one. This is because an FFT is used in the data processing of the mixed method, and the sampling number must be binary.

Experimental results

Stability of the system

Long- and short-term stability tests of the system were peformed in a circumstance without any temperature control or vibration isolation. In these tests, the output signals were sampled without rotating the cylindrical mirror. Therefore, the differential output of the mixed method calculated from these output data of the probes can be used to estimate the stability of the system.

Figures 15 and *16* show the long- and short-term stability of the system, respectively. In *Figure 15,* because the test term is short, and the influence of the thermal drift is small, the output of each probe is almost the same level as the probe reso-

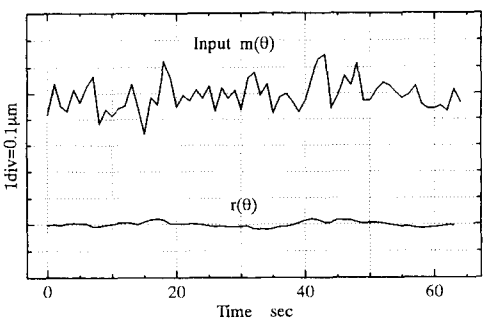

Figure 18 Stability of roundness measurement estimated from the drift data in *Figure 15*

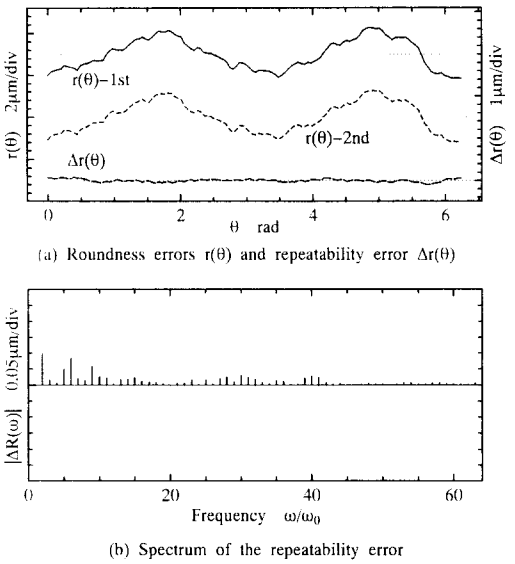

(a) Roundness errors r(θ) and repeatability error Δr(θ)

(b) Spectrum of the repeatability error

Figure 19 Measured roundness errors of sample 1

lution. The stability of the differential output of the mixed method is also the same level. On the other hand, in *Figure 16,* because the test term is long, and the influence of the thermal drift is large, the output of each probe varies much greater than the probe resolution. However, the differential output is almost the same level as that shown in *Figure 15.*

The stability of the roundness measurement can be estimated from that of the differential output through the data processing shown in *Figure 17. 64* datapoints of $m(\theta)$ shown in *Figure 15* were used to calculate the stability of the roundness measurement, and the calculated roundness error $r(\theta)$ is shown in *Figure 18* It can be seen that the stability is about 0.05 μm.

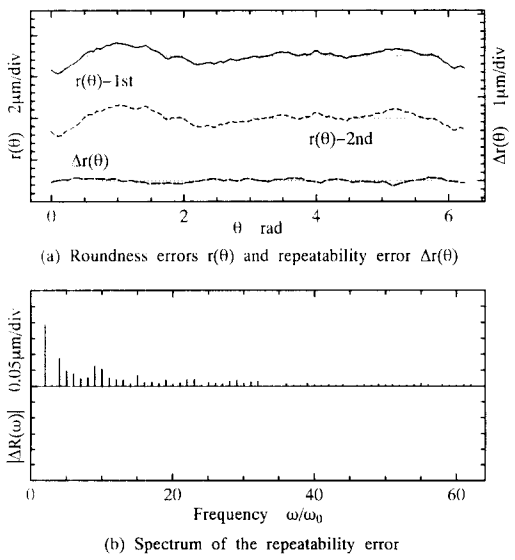

(a) Roundness errors r(θ) and repeatability error Δr(θ)

(b) Spectrum of the repeatability error

Figure 20 Measured roundness errors of sample 2

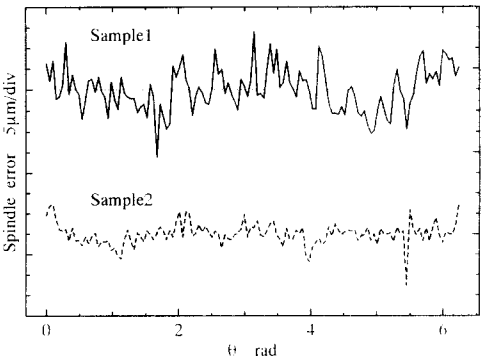

Figure 21 Measured spindle errors

Roundness measurement

Two cylindrical mirrors with the same diameter of 80 mm were measured. *Figure 19* shows the results of sample 1. The sampling number was 128, and the rotational speed was 43 rpm. *Figure 19a* shows the measured roundness errors of two separate measurements and the repeatability error between the two measured results. *Figure 19b* shows the spectrum of the repeatability error. The measured results of sample 2 are shown in *Figure 20.* It can be seen that the roundness error of sample 1 is about 12 μm, and that of sample 2 is about 8 μm. The repeatability error in the case of sample 1 is about 1 μm, and that in the case of Sample two is about 1.2 μm. The largest repeatability errors occurred at the second-order components, and the values in the cases of sample 1 and sample 2 are 0.1 μm and 0.2 μm, respectively. It can also be seen that the high-frequency components of the roundness error are measured with high repeatability. This confirmed the effectiveness of the mixed method.

The spindle error can be calculated by using the output of the displacement meter 1 and the

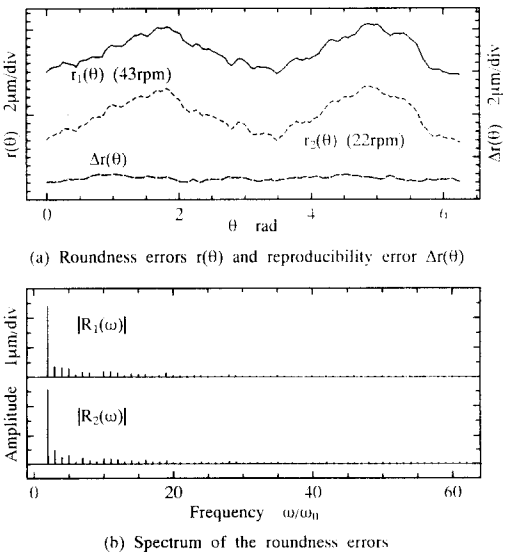

(a) Roundness errors r(θ) and reproducibility error Δr(θ)

(b) Spectrum of the roundness errors

Figure 22 Reproducibility error between the results at different rotational speeds

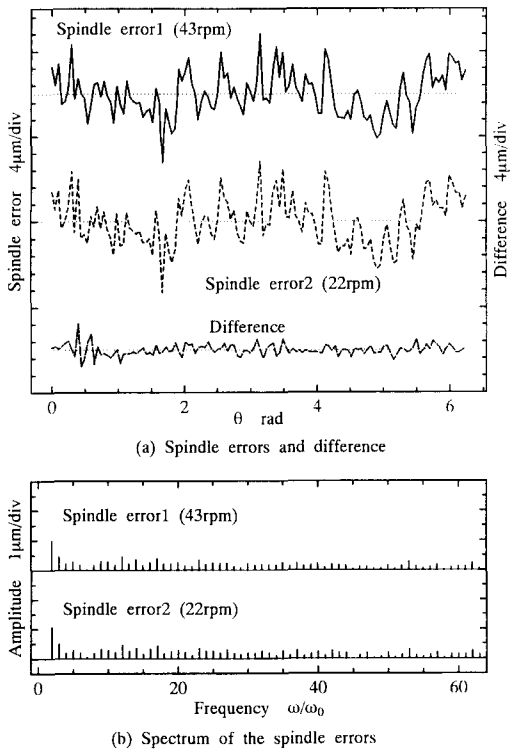

Figure 23 Difference between the measured spindle errors at different rotational speeds

evaluated roundness error. *Figure 21* shows the evaluated spindle errors. The spindle error in the case of sample 1 is about 30 μm, and that in the case of sample 2 is about 20 μm.

Sample 1 was also measured when the rotational speed was 22 rpm. *Figure 22* shows the results. $r1(\theta)$ is the roundness error measured at the rotational speed at 43 rpm, and $r2(\theta)$ is the roundness error measured at the rotational speed at 22 rpm. The reproducibility of the two measured results is about 2 μm. *Figure 23* shows the evaluated spindle error of each case. The difference between the two spindle errors is about 11 μm. The spindle error has no repeatability, because a ball bearing is used in the spindle. Comparing the results in *Figures 22* and *23,* it can be said that the roundness error and the spindle error are separated from each other.

Conclusions

1 A new multiprobe method for roundness measurements called the mixed method has been proposed. This method can separate roundness and spindle error completely and is well suited for measuring profiles that include high-frequency components.

2 An optical sensor that can detect the displacements at two points and one angle at one of the two points has been developed to perform roundness measurement with the mixed method. The resolution of the displacement meter and angle meter is 0.1 μm and 0.5 in. The possibility of applying an optical fiber system for power transmission to the sensor has also been confirmed.

3 A measurement system for roundness measurement using the mixed method has been constructed. Some techniques have been used to avoid the influence of the noise from the servomotor. The stability of the measurement system has been investigated. Estimating from the thermal drift characteristics, this system can measure roundness with a stability of 0.05 μm using the mixed method.

4 Roundness measurements have been performed, and the effectiveness of the mixed method was confirmed basically by the experimental results. The improvement of measurement accuracy will be done in our future work.

Acknowledgment

The authors thank Yoichi Shirahata of Tohoku Richo Co., Ltd and Taizou Touyama of Toyoda Machine Works, Ltd. for their cooperation in this study.

References

1 Whitehouse, D. J. "Some theoretical aspects of error separation techniques in surface metrology." *J Phy E: Scientific instruments,* 1976, **9,** 531–536

2 Donaldson, R. R. "A simple method for separating spindle error from test ball roundness error." *Ann CIRP,* 1972, **21,** 125–126

3 Chetwynd, D. G. and Siddall, G. J. "Improving the accuracy of roundness measurement." *J Phys E: Scientific instruments,* 1976, **9,** 537–544

4 Linxiang, Cao "The measuring accuracy of the multistep method in the error separation technique." *J Phys E: Scientific instruments,* 1988, **22,** 903–906

5 Nakamura, T., Funabashi, K. and Kosaka, K. "Measurement of form errors by phase difference method." *J JSME,* 1987 **53,** 716–720 (in Japanese)

6 Glenn, P. "Angstrom-level profilometry for submillimeter to meter scale surface errors." *Proc SPIE,* Advanced Optical Manufacturing and Testing, 1990. **1333,** 326–336

7 Ozono S., "On a new method of roundness measurement based on the three points method." *Proc international conference production engineering,* Tokyo, 1974, 457–462

8 Kakino, Y. and Kitazawa, J. "In situ measurement of cylindricity," *Ann CIRP, 1978,* **27,** 371–375

9 Shinno, H., Mitui, K., Tatsue, Y., Tanaka, N. and Tabata, T. "A new method for evaluating error motion of ultra precision spindle." *Ann CIRP,* 1987, **36,** 381–384

10 Zhang, H., Yun, H., Li, J. "an on-line measuring method of workpiece diameter based on the principle of 3-sensor error separation. *Proc IEEE 1990 national aerospace and electronics conference* 1990, **3,** 1308–1312

11 Fan, Y., Zhang, S. and Xu, W. "Kinematic and mathematical research on three-point method for in-process measurement and its applications in engineering." *Proc 7th international precision engineering seminar.* Kobe, Japan, 1993, 318–328

12 Kato, H., Song, R. and Nomura, Y. "In-situ measuring system of circularity using an industrial robot and a piezoactuator." *Int J JSPE,* 1991, **25,** 130–135

13 Ozono, S. and Hamano, Y. "On a new method of roundness measurement based on the three-point method (2nd report), Expanding the measurable maximum frequency," *Proc annual meeting of JSPE,* 1976, 503–504 (in Japanese)

14 Zhang, G. X. "Four-point method of roundness and spindle error measurements."' *Ann CIRP,* 1993, **42** 593–596

15 Gao, W. and Kiyono, S. "On-machine measurement of large mirror profile. *Proc ASPE 7th* Florida, 1992, 293–297

16 Hamming, R. W. *Digital filters.* New York: Prentice-Hall, 1977, Chapters 2 and 3, (translated into Japanese by H. Miyagawa and H. Jideki, Kagaku-Gijyutu Publishing, 1980).

17 Kiyono, S. and Gao W. "Profile measurement of machined surface with a new differential method." *Prec Eng* 1994, **16,** 212–218